



Published in final edited form as:

Nature. 2012 August 2; 488(7409): 43–48. doi:10.1038/nature11213.

## Novel mutations target distinct subgroups of medulloblastoma

Giles Robinson<sup>1,2,3,\*</sup>, Matthew Parker<sup>1,4,\*</sup>, Tanya A. Kranenburg<sup>1,2,\*</sup>, Charles Lu<sup>1,5</sup>, Xiang Chen<sup>1,4</sup>, Li Ding<sup>1,5,6</sup>, Timothy N. Phoenix<sup>1,2</sup>, Erin Hedlund<sup>1,4</sup>, Lei Wei<sup>1,4,7</sup>, Xiaoyan Zhu<sup>1,2</sup>, Nader Chalhoub<sup>1,2</sup>, Suzanne J. Baker<sup>1,2</sup>, Robert Huether<sup>1,4,8</sup>, Richard Kriwacki<sup>1,8</sup>, Natasha Curley<sup>1,2</sup>, Radhika Thiruvengadam<sup>1,2</sup>, Jianmin Wang<sup>1,9</sup>, Gang Wu<sup>1,4</sup>, Michael Rusch<sup>1,4</sup>, Xin Hong<sup>1,5</sup>, Jared Beckford<sup>1,9</sup>, Pankaj Gupta<sup>1,9</sup>, Jing Ma<sup>1,7</sup>, John Easton<sup>1,4</sup>, Bhavin Vadodaria<sup>1,4</sup>, Arzu Onar-Thomas<sup>1,10</sup>, Tong Lin<sup>1,10</sup>, Shaoyi Li<sup>1,10</sup>, Stanley Pounds<sup>1,10</sup>, Steven Paugh<sup>1,11</sup>, David Zhao<sup>1,9</sup>, Daisuke Kawachi<sup>1,12</sup>, Martine F. Roussel<sup>1,12</sup>, David Finkelstein<sup>1,4</sup>, David W. Ellison<sup>1,7</sup>, Ching C. Lau<sup>1,13</sup>, Eric Bouffet<sup>1,14</sup>, Tim Hassall<sup>1,15</sup>, Sridharan Gururangan<sup>1,16</sup>, Richard Cohn<sup>1,17</sup>, Robert S. Fulton<sup>1,5,6</sup>, Lucinda L. Fulton<sup>1,5,6</sup>, David J. Dooling<sup>1,5,6</sup>, Kerri Ochoa<sup>1,5,6</sup>, Amar Gajjar<sup>1,3</sup>, Elaine R. Mardis<sup>1,5,6,18</sup>, Richard K. Wilson<sup>1,5,6,19</sup>, James R. Downing<sup>1,7</sup>, Jinghui Zhang<sup>1,4</sup>, and Richard J. Gilbertson<sup>1,2,3</sup>

<sup>1</sup>St Jude Children's Research Hospital - Washington University Pediatric Cancer Genome Project

<sup>2</sup>Department of Developmental Neurobiology, St. Jude Children's Research Hospital, Memphis, Tennessee 38105, USA.

<sup>3</sup>Department of Oncology, St. Jude Children's Research Hospital, Memphis, Tennessee 38105, USA.

<sup>4</sup>Department of Computational Biology and Bioinformatics, St. Jude Children's Research Hospital, Memphis, Tennessee 38105, USA.

<sup>5</sup>The Genome Institute, Washington University School of Medicine in St. Louis, St. Louis, Missouri 63108, USA.

<sup>6</sup>Department of Genetics, Washington University School of Medicine in St. Louis, St. Louis, Missouri 63108, USA.

<sup>7</sup>Department of Pathology, St. Jude Children's Research Hospital, Memphis, Tennessee 38105, USA.

<sup>8</sup>Department of Structural Biology, St. Jude Children's Research Hospital, Memphis, Tennessee 38105, USA.

Users may view, print, copy, download and text and data- mine the content in such documents, for the purposes of academic research, subject always to the full Conditions of use: [http://www.nature.com/authors/editorial\\_policies/license.html#terms](http://www.nature.com/authors/editorial_policies/license.html#terms)

Correspondence should be addressed to: RJG (Richard.Gilbertson@stjude.org); JZ (Jinghui.Zhang@stjude.org); JRD (James.Downing@stjude.org); RKW (rwilson@wustl.edu)..

\*These authors contributed equally to the work.

**Author contributions.** G.R., M.P., T.A.K., C.L., X.C., L.D., T.N.P., E.H., W.L., X.Z., N.C., R.H., N.C., R.T., J.W., G.W., M.R., X.H., J.B., P.G., J.M., J.E., B.V., S.P., D.Z., D.K., D.F., contributed to the design and conduct of experiments and to the writing S.J.B., R.K., M.F.R., R.S.F., L.L.F., D.J.D., K.O., E.R.M., contributed to experimental design and to the writing A.G., D.W.E., C.C.L., E.B., T.H., S.G., R.C., provided clinical expertise. R.K.W., J.R.D., J.Z., and R.J.G., conceived the research and contributed to the design, direction and reporting of the study. No competing financial interests.

**Competing interests.** None.

**Supplementary Information.** Supplementary Information is available online.

<sup>9</sup>Department of Information Sciences, St. Jude Children's Research Hospital, Memphis, Tennessee 38105, USA.

<sup>10</sup>Department of Biostatistics, St. Jude Children's Research Hospital, Memphis, Tennessee 38105, USA.

<sup>11</sup>Department of Pharmaceutical Sciences, St. Jude Children's Research Hospital, Memphis, Tennessee 38105, USA.

<sup>12</sup>Department of Tumour Biology and Genetics, St. Jude Children's Research Hospital, Memphis, Tennessee 38105, USA.

<sup>13</sup>Texas Children's Cancer and Hematology Centers, 6701 Fannin St., Ste. 1420, Houston, TX 77030.

<sup>14</sup>The Hospital for Sick Children, 555 University Avenue, Toronto, Ontario, Canada, M5G 1X8.

<sup>15</sup>The Royal Children's Hospital, 50 Flemington Road, Parkville Victoria 3052 Australia.

<sup>16</sup>Duke University Medical Center, 102382, Durham, NC 27710

<sup>17</sup>The School of Women's and Children's Health, University of New South Wales, Kensington, NSW, Australia.

<sup>18</sup>Siteman Cancer Center, Washington University School of Medicine in St. Louis, St. Louis, Missouri 63108, USA.

<sup>19</sup>Department of Medicine, Washington University School of Medicine in St. Louis, St. Louis, Missouri 63108, USA.

## Summary

Medulloblastoma is a malignant childhood brain tumour comprising four discrete subgroups. To identify mutations that drive medulloblastoma we sequenced the entire genomes of 37 tumours and matched normal blood. One hundred and thirty-six genes harbouring somatic mutations in this discovery set were sequenced in an additional 56 medulloblastomas. Recurrent mutations were detected in 41 genes not yet implicated in medulloblastoma: several target distinct components of the epigenetic machinery in different disease subgroups, e.g., regulators of H3K27 and H3K4 trimethylation in subgroup-3 and 4 (e.g., *KDM6A* and *ZMYM3*), and CTNNB1-associated chromatin remodellers in WNT-subgroup tumours (e.g., *SMARCA4* and *CREBBP*). Modelling of mutations in mouse lower rhombic lip progenitors that generate WNT-subgroup tumours, identified genes that maintain this cell lineage (*DDX3X*) as well as mutated genes that initiate (*CDH1*) or cooperate (*PIK3CA*) in tumorigenesis. These data provide important new insights into the pathogenesis of medulloblastoma subgroups and highlight targets for therapeutic development.

---

Medulloblastoma is the most common malignant childhood brain tumor<sup>1</sup>. The disease includes four subgroups (Sonic Hedgehog (SHH)-subgroup, WNT-subgroup, subgroup-3 and subgroup-4) defined primarily by gene expression profiling that display differences in karyotype, histology and prognosis<sup>2</sup>. Studies of genetically engineered mice show these tumours arise from different cell types: SHH-subgroup medulloblastomas develop from committed cerebellar granule neuron progenitors (GNPs) in *Ptch1*<sup>+/-</sup> mice<sup>3,4</sup>; WNT-

subgroup tumours are generated by lower rhombic lip progenitors (LRLPs) in *Blbp-Cre* ; *Ctmb1<sup>+lox/Ex3</sup>* ; *Tp53<sup>flx/flx</sup>* mice<sup>5</sup>; while subgroup-3 medulloblastomas likely arise from an undefined class of cerebellar progenitors<sup>6</sup>. The identification of medulloblastoma subgroups has not changed clinical practice. All patients currently receive the same combination of surgery, radiation and chemotherapy. This aggressive treatment fails to cure two thirds of patients with subgroup-3 disease, and probably over-treats children with WNT-subgroup medulloblastoma who invariably survive with long term cognitive and endocrine side effects<sup>2,7</sup>. Drugs targeting the genetic alterations that drive each medulloblastoma subgroup could prove more effective and less toxic, but the identity of these alterations remains largely unknown.

## The genomic landscape of medulloblastoma

To identify genetic alterations that drive medulloblastoma, we performed whole genome sequencing (WGS) of DNA from 37 tumours and matched normal blood (discovery cohort). Tumours were subgrouped by gene expression (WNT-subgroup, n=5; SHH-subgroup, n=5; subgroup-3, n=6; subgroup-4, n=19; 'unclassified' [profiles not available], n=2. Figure 1; Supplementary Figures 1-3 and Supplementary Table 1). Validation of all putative somatic alterations including single nucleotide variations (SNVs), insertion/deletions (indels) and structural variations (SVs) identified by CREST<sup>8</sup>, was conducted for 12 tumours using custom capture arrays and Illumina-based DNA sequencing (Supplementary Table 2). Putative coding alterations and SVs were validated in the remaining 25 'discovery cohort' cases by polymerase chain reaction and Sanger-based sequencing. Mutation frequency was determined in a separate 'validation cohort' of 56 medulloblastomas (WNT-subgroup, n=6; SHH-subgroup, n=8; subgroup-3, n=11; subgroup-4, n=19; unclassified, n=12; Figure 1, Supplementary Table 1).

WGS of the 'discovery cohort' detected 22,887 validated or high-quality somatic sequence mutations (SNVs and indels), 536 validated or curated SVs, and 5,802 copy number variations (CNVs, 92% concordant with 6.0 SNP mapping arrays; Supplementary Tables 3-6, Supplementary Figures 4-7). In all but five tumours with the highest mutation rates, >50% of SNVs were C>T/G>A transitions (Supplementary Figure 8). The mean missense:silent mutation ratio was 3.6:1 and 40% of all missense mutations were predicted to be deleterious, suggesting a selective pressure for SNVs that impact protein coding (Supplementary Table 5). Global patterns of total SNVs and amplifications varied significantly among medulloblastoma subgroups, even when corrected for age and sex, supporting the notion that these tumours are distinct pathological entities (Figure 1, Supplementary Figure 6). Custom capture-based analysis of the allele frequency of all somatic mutations in 12 medulloblastomas allowed us to predict the ancestry of certain genetic alterations, suggesting that aneuploidy precedes widespread sequence mutation in medulloblastomas with highly mutated genomes (Supplementary Figures 9-11).

## Novel copy number variations, structural alterations and heritable mutations are rare in medulloblastoma

The repertoire of focally amplified or deleted genes appears to be very limited in medulloblastoma. We detected expected<sup>2</sup> gains of *MYC*, *MYCN* and *OTX2* in subgroup-3 and 4, but no novel recurrent amplifications (Figure 1, Supplementary Figure 12, Supplementary Table 7). In keeping with recent reports<sup>9</sup>, high-level amplification of *MYCN* in subgroup-3 sample #16 (sample numbering as Figure 1) was generated by chromothripsis; although chromothripsis was observed infrequently (n=2/37 of ‘discovery cohort’; Supplementary Figure 13).

Focal homo- or heterozygous deletion of genes previously implicated in medulloblastoma were also detected (e.g., *PTCH1*, *PTEN*, Figure 1)<sup>10,11</sup> but novel recurrent focal deletions were rare. Three subgroup-4 tumours (#11-13) and one unclassified tumour, deleted *DDX31*, *AK8* and *TSC1* at 9q34.14 in concert with *OTX2* amplification, suggesting these alterations are cooperative (P<0.0005, Fisher’s exact). The breakpoint in this deletion occurs in *DDX31* and two samples contained a missense mutation (subgroup-4 #15) and complex rearrangement (unidentified case SJMB026) in this gene, suggesting *DDX31* is the target of these alterations (Supplementary Figure 14).

Over 50% of SVs detected by WGS broke the coding region of at least one gene, but less than 2% (n=6/314, excluding two tumours with excessive SVs) encode potential in-frame fusion proteins (Supplementary Figure 15); none affect the same gene or signal pathway. Therefore, fusion proteins are likely to be an uncommon transforming mechanism in medulloblastoma.

Although germline mutations in *TP53*, *PTCH1*, *APC*, and *CREBBP*, predispose to medulloblastoma<sup>11-14</sup>, only 23 mutations previously associated with cancer were detected in ‘discovery cohort’ germlines: only one of these - in a known case of Turcot’s syndrome - was accompanied with a somatic mutation (germline *APC* Y935\*/somatic deletion: WNT-subgroup #11, Supplementary Table 8). Thus, inherited forms of medulloblastoma appear to be rare in our cohort.

## Novel recurrent sequence mutations target distinct medulloblastoma subgroups

Since SVs and CNVs are unlikely to drive most medulloblastomas, we looked to see if recurrent (>2 samples), somatic SNVs and/or indels might target discrete genes and pathways. This analysis identified 49 genes, across all 93 tumors, that were targeted by non-silent, recurrent, somatic mutations: 84% (n=41/49) are not yet implicated in medulloblastoma (Supplementary Tables 9 and 10). Several of these congregated in disease subgroups and converged on specific cell pathways (Figure 1; Supplementary Figure 8 and Table 11).

## Writing, reading and erasing of histone methylation is deregulated in subgroup-3 and 4 medulloblastomas

The H3K27 trimethyl mark (H3K27me<sub>3</sub>) represses lineage specific genes in stem cells (Supplementary Figure 8)<sup>15</sup>. H3K27me<sub>3</sub> is written by the polycomb repressive complex 2 (PRC2) that includes the methylase EZH2<sup>16,17</sup>, and erased during differentiation by the demethylase KDM6A<sup>18</sup>. As H3K27me<sub>3</sub> is erased, chromatin remodelers recruited to H3K4me<sub>3</sub> promote differentiation e.g., CHD7<sup>19,20</sup>. This process is tightly controlled during development and deregulated in cancers: *EZH2* is mutated in lymphomas<sup>21</sup>, and upregulated in breast<sup>22</sup> and prostate<sup>23</sup> cancer; while biallelic inactivation of *KDM6A* (Xp11.2) or *KDM6A* and its paralog *UTY* (Yq11), occurs in adult female and male cancers, respectively<sup>24</sup>.

Hypergeometric distribution analyses revealed selective mutation of histone modifiers in subgroup-3 and 4 medulloblastomas (Supplementary Table 11). Six subgroup-4, one subgroup-3, and one unclassified medulloblastoma contained novel inactivating mutations in *KDM6A* (Figures 1 and 2; Supplementary Figures 8 and 16). The single female with a *KDM6A* splice site mutation deleted the second allele that escapes X inactivation<sup>25</sup> (subgroup-4 #15), and 57% (n=4/7) of *KDM6A*-mutant male medulloblastomas deleted chromosome Y, compared with only 6% (n=3/51) of male, *KDM6A* wild-type tumours (P<0.005, Fisher's exact; Figure 1). Thus, a two-hit model of *KDM6A-UTY* tumour suppression appears to operate in subgroup-4 medulloblastomas. Notably, mutations in six other KDM family members (*KDM1A*, *KDM3A*, *KDM4C*, *KDM5A*, *KDM5B* and *KDM7A*) were detected exclusively in subgroup-3 and 4 tumours, implicating broad disruption of lysine demethylation in these medulloblastomas (Figure 1, Supplementary Table 11; Supplementary Figure 16).

Subgroup-3 and 4 medulloblastomas also gained and overexpressed *EZH2* (7q35-34) that writes H3K27me<sub>3</sub>, and contained novel inactivating mutations in effectors and regulators of the H3K4me<sub>3</sub> mark<sup>26</sup> (Figure 2a; Supplementary Figure 8). Gain of 7q was significantly enriched among subgroup-3 and 4 medulloblastomas (P<0.005 Fisher's exact) and correlated directly with *EZH2* expression. Indeed, *EZH2* was the 8<sup>th</sup> most significantly overexpressed gene on chromosome 7 among subgroup-3 and 4 medulloblastomas that gained chromosome 7q relative to those with diploid chromosome 7 (P<0.005, Bonferroni correction). Nonsense and frameshift mutations were detected in *CHD7* in four subgroup-3 and 4 tumours. *ZMYM3* (Xq13.1) that participates in a protein complex with *KDM1A* to regulate gene expression at the H3K4me<sub>3</sub> mark<sup>27</sup> was targeted by novel frameshift, nonsense and missense mutations in three male subgroup-4 medulloblastomas. All three tumours with mutations in *ZMYM3* also mutated *KDM6A* (subgroup-4 #19, 20) or *KDM1A* (subgroup-4 #21) suggesting these alterations are cooperative. Remarkably, *KDM6A*, *CHD7* and *ZMYM3* mutations were confined to subgroup-3 and 4, and clustered in samples with sub-median *EZH2* expression levels (Figure 2a; P<0.05, Fisher's exact). These data suggest that subgroup-3 and 4 medulloblastomas retain a stem-like epigenetic state by aberrantly writing (*EZH2* upregulation) or preserving (*KDM6A-UTY* inactivation) H3K27me<sub>3</sub>, or disrupting H3K4me<sub>3</sub> associated transcription (*CHD7* and *ZMYM3* inactivation). Indeed, human and mouse subgroup-3 and 4 medulloblastomas contained significantly more

H3K27me3 than did WNT or SHH-subgroup tumours (Figure 2b). Thus, gain of *EZH2* and loss of *KDM6A* likely maintains H3K27me3 in subgroup-3 and 4 medulloblastomas.

Finally, we looked to see if the differential expression of H3K27me3 among medulloblastoma subgroups reflects ancestral chromatin marking in the progenitors that generate these tumours (Figure 2b). Relatively low levels of H3K27me3 were detected in LRLPs and committed GNPs that generate WNT and SHH-subgroup medulloblastomas respectively<sup>3-5</sup>, potentially explaining why mutations that preserve this epigenetic mark are absent from these tumours. We recently showed that subgroup-3 medulloblastomas arise from a rare fraction of cerebellar progenitors<sup>6</sup>. We are currently investigating if these progenitors are found among the H3K27me<sup>3</sup> positive cells seen in the external germinal layer (Figure 2b).

### **Novel mutations in WNT-subgroup medulloblastomas target CTNNB1-associated chromatin remodelers and regulators of LRLPs**

WNT-subgroup medulloblastomas contained mutations in epigenetic regulators that are different to those seen in subgroup-3 and 4 disease. CTNNB1, the principal effector of the WNT pathway, forms a transcription factor with the T cell factor/lymphoid enhancer factor (TCF/LEF)<sup>28</sup>. The c-terminus of CTNNB1 then recruits a series of protein complexes that remodel chromatin and promote transcription at WNT-responsive genes (Supplementary Figure 8). These include: histone acetyltransferases (e.g., CREBBP and TRRAP-TIP60 complexes)<sup>28,29</sup>; ATPases of the SWI/SNF family (e.g., SMARCA4)<sup>30</sup>; and the Mediator complex that coordinates RNA polymerase II placement (e.g., MED13)<sup>31</sup>. As expected, >70% (n=8/11) of WNT-medulloblastomas contained mutations that stabilise CTNNB1 (Figure 1 and Supplementary Figure 8; P<0.0001, Fishers exact)<sup>32,33</sup>. A single subgroup-3 case (#5) also mutated *CTNNB1*, but this mutation has not been reported in cancer, did not upregulate nuclear CTNNB1 (Figure 1) and is of unclear significance. Remarkably, six WNT-subgroup medulloblastomas mutated chromatin modifiers that are recruited to TCF/LEF WNT-responsive genes by CTNNB1 (Figure 1, Supplementary Figure 8): four WNT-subgroup tumours contained heterozygous missense mutations in the helicase domain of *SMARCA4* (P<0.002, Fisher's exact); two samples, including one with a *SMARCA4* mutation (#5), contained nonsense mutations in *CREBBP* (WNT-subgroup enrichment P<0.02, Fisher's exact); and missense mutations in *TRRAP* and *MED13* were detected in a single WNT-subgroup medulloblastoma each. Thus, in addition to stabilization of CTNNB1, the development of WNT-subgroup medulloblastoma may require disruption of chromatin remodeling at WNT-responsive genes.

A small number of WNT-subgroup medulloblastomas lack mutations in *CTNNB1* or *APC*, suggesting alternative mechanisms drive aberrant WNT-signals in these tumours. Three WNT-subgroup medulloblastomas in our series contained wild-type *CTNNB1* (#1, 10 and 11, Figure 1). Sample #11 inactivated *APC* as the sole case of Turcot's Syndrome in our study, but this tumour and sample #10 also contained novel missense mutations in *CDH1* (R63G, V329F; Figure 1 WNT-subgroup enrichment P<0.05, Fisher's exact). CDH1 sequesters CTNNB1 at the cell membrane<sup>34</sup>, and mutations that disrupt this interaction promote WNT signaling in adult cancers<sup>35,36</sup>. The functional consequences of CDH1<sup>R63G</sup>



and CDH1<sup>V329F</sup> remain to be determined, but their restriction to WNT-subgroup tumours; mutual exclusivity with *CTNNB1* mutations; and adjacency to residues mutated in breast cancer (<http://www.sanger.ac.uk/genetics/CGP/cosmic/>), suggest these might promote aberrant WNT signals in medulloblastoma.

We showed previously that mutant *Ctnnb1* initiates WNT-subgroup medulloblastoma by arresting the migration of LRLPs from the embryonic dorsal brainstem to the pontine grey nucleus (PGN)<sup>5</sup>. Therefore, to test if disruption of CDH1 might substitute for mutant *CTNNB1* in medulloblastoma, we used shRNAs to knock down *Cdh1* in embryonic day (E) 14.5 mouse LRLPs (Figure 3a to c). Deletion of *Cdh1* expression upregulated *Tcf/Lef* mediated gene transcription in LRLPs and more than doubled their self-renewal capacity (Figure 3b). Furthermore, *in utero* electroporation of LRLPs with *Cdh1* shRNAs impeded their migration from the dorsal brainstem to the PGN with an efficiency similar to that of mutant *Ctnnb1* (Figure 3d,e; see Supplementary Methods). These data support the hypothesis that *CDH1* suppresses the formation of WNT-subgroup medulloblastoma by regulating WNT-signals in LRLPs.

WNT-subgroup medulloblastomas were also enriched for novel, recurrent somatic missense mutations in the DEAD-Box RNA helicase *DDX3X* at Xp11.3 ( $P < 0.0001$ , Fisher's exact; Figure 1). *DDX3X* regulates several critical cell processes including chromosome segregation<sup>37</sup>, cell cycle progression<sup>38</sup>, gene transcription and translation<sup>39</sup>. Previously reported cancer associated mutations in *DDX3X* disrupt the ATPase activity of the protein, but seven of eight mutations identified in our series clustered in the DEAD-box domain (Supplementary Information; Supplementary Figure 8). Structural modeling predicts that these mutations interfere with nucleic acid binding, possibly altering specificity and/or affinity for RNA substrates, rather than inactivating *DDX3X* (Supplementary Figures 17-22). Indeed, the wild-type allele of *DDX3X* that escapes X inactivation<sup>25</sup> was retained by two of three *DDX3X*-mutant female medulloblastomas, and knock-down of *Ddx3x* halved the self-renewal rate of mouse LRLPs, suggesting this protein is important for the proliferation and/or maintenance of the LRLP lineage (Figure 3b).

To better understand the role of *DDX3X* in WNT-subgroup medulloblastoma, we employed our *in utero* migration assay to assess the impact of *Ddx3x* shRNAs, mutant-*Ddx3x*<sup>T275M</sup> (identified in WNT-sample #9) or mutant-*Ddx3x*<sup>G325E</sup> (WNT-sample #8) on LRLPs. Remarkably, while *Ddx3x* shRNAs were expressed abundantly in E14.5 brainstem cells within 48 hours of electroporation, <0.5% of *Ddx3x*- shRNA-positive cells were present by postnatal day 1, confirming the critical importance of this gene to maintain the LRLP lineage (Figure 3d,e). In stark contrast, mice electroporated with either mutant-*Ddx3x*<sup>T275M</sup> or *Ddx3x*<sup>G325E</sup> consistently contained ~50% more labeled cells at postnatal day (P) 1 than did controls, although these cells migrated normally (Figure 3d,e and data not shown). Thus, mutations in *DDX3X* may contribute to WNT-subgroup medulloblastoma by increasing LRLP proliferation rather than perturbing the migration of their daughters. Notably, comparable knock-down *in utero* of *Mil2*, *Gabrg1*, and *Kdm6a* that were selectively mutated in non-WNT medulloblastomas had no apparent impact on LRLPs; supporting the value of our assay for assessing WNT-subgroup specific mutations and underscoring the importance of cell context for functional studies of genes mutated in cancer subgroups.

## PIK3CA mutations promote but don't initiate WNT-subgroup medulloblastoma

Cancer-associated, activating mutations in *PIK3CA* were detected in a single case each of WNT (*PIK3CA*<sup>Q546K</sup>), SHH (*PIK3CA*<sup>H1047R</sup>) and subgroup-4 (*PIK3CA*<sup>N345K</sup>) medulloblastoma (Figure 1; Supplementary Figure 23). Although *PIK3CA* mutations are common in adult cancers<sup>40</sup> and reported in medulloblastoma<sup>41</sup>, their role in tumorigenesis remains controversial. In particular it is not known if these mutations initiate or progress cancer. To test this, we generated mice that express a conditional allele of the *Pik3ca*<sup>E545K</sup> mutation. Mice harboring *Pik3ca*<sup>E545K</sup> or *Pik3ca*<sup>E545K</sup> and *Tp53*<sup>flx/flx</sup> were bred with *Blbp-Cre* that drives efficient recombination in LRLPs<sup>5</sup>. *Blbp-Cre*; *Pik3ca*<sup>E545K</sup> mice, with or without *Tp53*<sup>flx/flx</sup>, survived tumour free for a median of 212 days with no evidence of aberrant LRLP migration (Figure 4a and data not shown). In stark contrast, 100% (n=11/11) of *Blbp-Cre*; *Ctnnb1*<sup>+lox(Ex3)</sup>; *Tp53*<sup>+flx</sup>; *Pik3ca*<sup>E545K</sup> mice developed WNT-subgroup medulloblastomas by 3 months of age: only 4% (n=2/54) of *Blbp-Cre*; *Ctnnb1*<sup>+lox(Ex3)</sup>; *Tp53*<sup>+flx</sup> mice develop WNT-medulloblastoma by 11 months (Figure 4a,b). *Pik3ca* wild-type and mutant mouse medulloblastomas displayed similar 'classic' histologies and nuclear *Ctnnb1*<sup>+</sup>, but *Pik3ca*<sup>E545K</sup> mutant tumors contained greater AKT pathway activity as measured by pS6 and p4EBP1 immunostaining. Thus mutations in *PIK3CA* likely activate the AKT pathway to progress, rather than initiate, WNT-medulloblastoma.

## SHH-subgroup medulloblastomas

Four of 13 SHH-subgroup medulloblastomas contained expected biallelic inactivating alterations in *SUFU* or *PTCH1*. What drives aberrant SHH-signals in the remaining cases remains unclear. These tumours contained mutations in *MLL2*, *TP53*, and *PTEN* that have been reported previously in medulloblastoma<sup>42</sup>; but these mutations occur in other subgroups and are not known to activate SHH signals. Two SHH-subgroup tumours (#11 and 12) contained identical novel T48M mutations in gamma-aminobutyric acid (GABA) A receptor, gamma 1 that is predicted to be deleterious (Figure 1, Supplementary Table 9). Disruption of GABA<sub>A</sub> receptors can enhance neural stem cell proliferation<sup>43</sup>, suggesting these mutations might deregulate the proliferation of GNP that generate SHH-subgroup medulloblastomas.

## Discussion

We have identified several, new, recurrent, somatic mutations in specific subgroups of medulloblastoma. Alterations affecting *EZH2*, *KDM6A*, *CHD7* and *ZMYM3* appear to disrupt chromatin marking of genes in subgroup-3 and 4 tumours. Further epigenetic studies will be required to uncover the identity of these genes, but evidence suggests these may include *OTX2*, *MYC* and *MYCN*<sup>44,45</sup>. Since amplification of these genes was detected almost exclusively in subgroup-3 and 4 tumours that lacked mutations in *KDM6A*, *CHD7* or *ZMYM3*, it is tempting to speculate that these genetic alterations target common transforming pathways. A recent study detected recurrent mutations in three other chromatin remodelers in medulloblastoma<sup>42</sup>: *SMARCA4*, *MLL2* and *MLL3*, but this study did not include details of tumour subgroup. Here, we show that mutations in *SMARCA4*, *CREBBP*, *TRRAP* and *MED13* are enriched in WNT-subgroup medulloblastomas; thereby uncovering potential cooperative mutations in chromatin remodelers and their binding-partner



oncogene, CTNNB1. Thus, disruptions in the epigenetic machinery of medulloblastoma are likely to be subgroup specific and may cooperate with other oncogenic mutations. The low incidence of *MLL2* mutations detected in our study relative to Parsons et al.,<sup>42</sup> likely reflects differences in our study populations (see Supplementary Results).

Although medulloblastoma is more prevalent in males, especially subgroup-3 and 4 disease<sup>46</sup>, the reason for this sex bias is unknown. One potential explanation is the location of medulloblastoma oncogenes or tumour suppressor genes on chromosome X<sup>47</sup>. Three of the most recurrently mutated genes detected in our study are located on chromosome X, of which two (*ZMYM3* and *KDM6A*) were observed almost exclusively in males. Mutation of these genes might explain some of the male sex-bias in medulloblastoma. The third mutated X chromosome gene, *DDX3X*, is more likely to be a WNT-medulloblastoma oncogene. Three of four female medulloblastomas carried heterozygous mutations in *DDX3X* that escapes X inactivation<sup>25</sup> and our functional data indicate that mutations in this gene provide a proliferative advantage to LRLPs that generate these tumours.

Our findings also have important implications for drug development. Inhibitors of the epigenetic machinery, especially those that maintain H3K27me3 e.g., EZH2 methylases, may be useful treatments of subgroup-3 and 4 disease. These tumours include the most aggressive forms of medulloblastoma for which treatment options are limited. Mutations that activate PIK3CA and *DDX3X* in WNT-subgroup tumors might also be targeted with novel therapeutic strategies<sup>48,49</sup>. Future clinical trials of drugs that target these mutant proteins must recruit the appropriate patient populations, since we show mutations display subgroup-specificity in medulloblastoma. Our accurate mouse models of WNT, SHH and subgroup-3 medulloblastoma should help considerably with future studies of the biological and therapeutic significance of the novel genetic alterations described in this study.

## Methods summary

Human tumour and matched blood samples were obtained with informed consent through an institutional review board approved protocol at St Jude Children's Research Hospital. Whole genome sequencing (WGS) and analysis of WGS data were performed as previously described<sup>50</sup>. Details of sequence coverage, custom capture and other validation procedures are provided in Supplementary Information (Supplementary Tables 12-15). Sequence and SNP array data were deposited in dbGaP (dbGaP accession number: phs000409, SRA accession number: SRP008292). Immunohistochemistry and immunofluorescence of human and mouse tissues were performed using routine techniques and primary antibodies of the appropriate tissues as described (Supplementary Methods). Medulloblastoma mRNA and DNA profiles were generated using Affymetrix U133v2 and SNP 6.0 arrays, respectively (Supplementary Methods). Reverse transcriptase Real Time-PCR analysis of genes targeted in mouse LRLPs by shRNAs were performed as described previously<sup>32</sup>. LRLPs were isolated and transduced with indicated lentiviruses in stem cell cultures or targeted *in utero* with shRNAs or mutant cDNA sequences by electroporation as described (Supplementary Information)<sup>5</sup>. Mice harbouring a cre-inducible *Pik3ca*<sup>E545K</sup> allele were generated using homologous recombination: A lox-puro-STOP-lox cassette was introduced immediately upstream of the exon containing the initiation codon, exon 9 was replaced with an exon

containing the E545K mutation. *Pik3ca*<sup>E545K</sup> mice were bred with *Blbp-Cre*, *Ctnnb1*<sup>lox(ex3)/lox(ex3)</sup> and *Tp53*<sup>flx/flx</sup> mice to generate progeny of the appropriate genotype and subjected to clinical surveillance.

## Supplementary Material

Refer to Web version on PubMed Central for supplementary material.

## Acknowledgements

This research was supported as part of the St. Jude Children's Research Hospital, Washington University Pediatric Cancer Genome Project. This work was supported by grants from the National Institutes of Health (R01CA129541, P01CA96832 and P30CA021765, R.J.G), the Collaborative Ependymoma Research Network (CERN), Musicians against Childhood Cancer (MACC), The Noyes Brain Tumour Foundation, and by the American Lebanese Syrian Associated Charities (ALSAC). We are grateful to Sally Temple for the generous gift of reagents and the staff of the Hartwell Center for Bioinformatics and Biotechnology and ARC at St Jude Children's Research Hospital for technical assistance.

## References

1. CBTRUS. Statistical Report: Primary Brain Tumors in the United States, 1995-1999. Central Brain Tumor Registry of the United States; Hinsdale, IL: 2006. 2002
2. Taylor MD, et al. Molecular subgroups of medulloblastoma: the current consensus. *Acta Neuropathol.* 2012; 123:465–472. Epub 2011 Dec 2012. [PubMed: 22134537]
3. Schuller U, et al. Acquisition of granule neuron precursor identity is a critical determinant of progenitor cell competence to form Shh-induced medulloblastoma. *Cancer Cell.* 2008; 14:123–134. [PubMed: 18691547]
4. Yang ZJ, et al. Medulloblastoma can be initiated by deletion of Patched in lineage-restricted progenitors or stem cells. *Cancer Cell.* 2008; 14:135–145. [PubMed: 18691548]
5. Gibson P, et al. Subtypes of medulloblastoma have distinct developmental origins. *Nature.* 2010; 468:1095–1099. [PubMed: 21150899]
6. Kawauchi D, et al. A mouse model of the most aggressive subgroup of human medulloblastoma. *Cancer Cell.* 2012; 21:168–180. [PubMed: 22340591]
7. Mulhern RK, et al. Neurocognitive Consequences of Risk-Adapted Therapy for Childhood Medulloblastoma. *Journal of Clinical Oncology.* 2005; 23:5511–5519. [PubMed: 16110011]
8. Wang J, et al. CREST maps somatic structural variation in cancer genomes with base-pair resolution. *Nat Meth.* 2011; 8:652–654.
9. Rausch T, et al. Genome Sequencing of Pediatric Medulloblastoma Links Catastrophic DNA Rearrangements with TP53 Mutations. *Cell.* 2012; 148:59–71. doi:10.1016/j.cell.2011.12.013. [PubMed: 22265402]
10. Castellino RC, et al. Heterozygosity for Pten Promotes Tumorigenesis in a Mouse Model of Medulloblastoma. *PLoS One.* 2010; 5:e10849. [PubMed: 20520772]
11. Hahn H, et al. Mutations of the human homolog of Drosophila patched in the nevoid basal cell carcinoma syndrome. *Cell.* 1996; 85:841–851. [PubMed: 8681379]
12. Malkin D, et al. Germ line p53 mutations in a familial syndrome of breast cancer, sarcomas, and other neoplasms. *Science.* 1990; 250:1233–1238. [PubMed: 1978757]
13. Hamilton SR, et al. The molecular basis of Turcot's syndrome. *N Engl J Med.* 1995; 332:839–847. [PubMed: 7661930]
14. Taylor MD, et al. Medulloblastoma in a child with Rubenstein-Taybi Syndrome: case report and review of the literature. *Pediatr Neurosurg.* 2001; 35:235–238. [PubMed: 11741116]
15. Mikkelsen TS, et al. Genome-wide maps of chromatin state in pluripotent and lineage-committed cells. *Nature.* 2007; 448:553–560. [PubMed: 17603471]

16. Cao R, et al. Role of histone H3 lysine 27 methylation in Polycomb-group silencing. *Science*. 2002; 298:1039–1043. Epub 2002 Sep 10. [PubMed: 12351676]
17. Czermin B, et al. Drosophila Enhancer of Zeste/ESC Complexes Have a Histone H3 Methyltransferase Activity that Marks Chromosomal Polycomb Sites. *Cell*. 2002; 111:185–196. [PubMed: 12408863]
18. Agger K, et al. UTX and JMJD3 are histone H3K27 demethylases involved in HOX gene regulation and development. *Nature*. 2007; 449:731–734. [PubMed: 17713478]
19. Schnetz MP, et al. Genomic distribution of CHD7 on chromatin tracks H3K4 methylation patterns. *Genome Research*. 2009; 19:590–601. [PubMed: 19251738]
20. Sauvageau M, Sauvageau G. Polycomb Group Proteins: Multi-Faceted Regulators of Somatic Stem Cells and Cancer. *Cell Stem Cell*. 2010; 7:299–313. [PubMed: 20804967]
21. Morin RD, et al. Somatic mutations altering EZH2 (Tyr641) in follicular and diffuse large B-cell lymphomas of germinal-center origin. *Nat Genet*. 2010; 42:181–185. [PubMed: 20081860]
22. Kleer CG, et al. EZH2 is a marker of aggressive breast cancer and promotes neoplastic transformation of breast epithelial cells. *Proceedings of the National Academy of Sciences*. 2003; 100:11606–11611.
23. Varambally S, et al. The polycomb group protein EZH2 is involved in progression of prostate cancer. *Nature*. 2002; 419:624–629. [PubMed: 12374981]
24. van Haaften G, et al. Somatic mutations of the histone H3K27 demethylase gene UTX in human cancer. *Nat Genet*. 2009; 41:521–523. [PubMed: 19330029]
25. Yang F, Babak T, Shendure J, Distèche CM. Global survey of escape from X inactivation by RNA-sequencing in mouse. *Genome Research*. 2010; 20:614–622. [PubMed: 20363980]
26. Christensen J, et al. RBP2 Belongs to a Family of Demethylases, Specific for Tri- and Dimethylated Lysine 4 on Histone 3. *Cell*. 2007; 128:1063–1076. [PubMed: 17320161]
27. Lee MG, Wynder C, Cooch N, Shiekhhattar R. An essential role for CoREST in nucleosomal histone 3 lysine 4 demethylation. *Nature*. 2005; 437:432–435. [PubMed: 16079794]
28. Mosimann C, Hausmann G, Basler K. [beta]-Catenin hits chromatin: regulation of Wnt target gene activation. *Nat Rev Mol Cell Biol*. 2009; 10:276–286. [PubMed: 19305417]
29. Hecht A, Vleminckx K, Stemmler MP, van Roy F, Kemler R. The p300/CBP acetyltransferases function as transcriptional coactivators of [beta]-catenin in vertebrates. *EMBO J*. 2000; 19:1839–1850. [PubMed: 10775268]
30. Barker N, et al. The chromatin remodelling factor Brg-1 interacts with [beta]-catenin to promote target gene activation. *EMBO J*. 2001; 20:4935–4943. [PubMed: 11532957]
31. Carrera I, Janody F, Leeds N, Duveau F, Treisman JE. Pygopus activates Wingless target gene transcription through the mediator complex subunits Med12 and Med13. *Proceedings of the National Academy of Sciences*. 2008; 105:6644–6649.
32. Thompson MC, et al. Genomics identifies medulloblastoma subgroups that are enriched for specific genetic alterations. *J Clin Oncol*. 2006; 24:1924–1931. Epub 2006 Mar 19. [PubMed: 16567768]
33. Kool M, et al. Integrated genomics identifies five medulloblastoma subtypes with distinct genetic profiles, pathway signatures and clinicopathological features. *PLoS One*. 2008; 3:e3088. [PubMed: 18769486]
34. Orsulic S, Huber O, Aberle H, Arnold S, Kemler R. E-cadherin binding prevents beta-catenin nuclear localization and beta-catenin/LEF-1-mediated transactivation. *Journal of Cell Science*. 1999; 112:1237–1245. [PubMed: 10085258]
35. Risinger JI, Berchuck A, Kohler MF, Boyd J. Mutations of the E-cadherin gene in human gynecologic cancers. *Nat Genet*. 1994; 7:98–102. [PubMed: 8075649]
36. Becker K-F, et al. E-Cadherin Gene Mutations Provide Clues to Diffuse Type Gastric Carcinomas. *Cancer Research*. 1994; 54:3845–3852. [PubMed: 8033105]
37. Pek JW, Kai T. DEAD-box RNA helicase Belle/DDX3 and the RNA interference pathway promote mitotic chromosome segregation. *Proc Natl Acad Sci U S A*. 2011; 108:12007–12012. [PubMed: 21730191]

38. Lai MC, Chang WC, Shieh SY, Tarn WY. DDX3 regulates cell growth through translational control of cyclin E1. *Mol Cell Biol.* 2010; 30:5444–5453. [PubMed: 20837705]
39. Schroder M. Human DEAD-box protein 3 has multiple functions in gene regulation and cell cycle control and is a prime target for viral manipulation. *Biochem Pharmacol.* 2010; 79:297–306. [PubMed: 19782656]
40. Samuels Y, et al. High frequency of mutations of the PIK3CA gene in human cancers. *Science.* 2004; 304:554. [PubMed: 15016963]
41. Broderick DK, et al. Mutations of PIK3CA in anaplastic oligodendrogliomas, high-grade astrocytomas, and medulloblastomas. *Cancer Res.* 2004; 64:5048–5050. [PubMed: 15289301]
42. Parsons DW, et al. The genetic landscape of the childhood cancer medulloblastoma. *Science.* 2011; 331:435–439. [PubMed: 21163964]
43. Andang M, et al. Histone H2AX-dependent GABAA receptor regulation of stem cell proliferation. *Nature.* 2008; 451:460–464. [PubMed: 18185516]
44. Pasini D, et al. Coordinated regulation of transcriptional repression by the RBP2 H3K4 demethylase and Polycomb-Repressive Complex 2. *Genes & Development.* 2008; 22:1345–1355. [PubMed: 18483221]
45. Khan A, Shover W, Goodliffe JM. Su(z)2 Antagonizes Auto-Repression of Myc in *Drosophila*, Increasing Myc Levels and Subsequent Trans-Activation. *PLoS One.* 2009; 4:e5076. [PubMed: 19333393]
46. Northcott PA, et al. Medulloblastoma comprises four distinct molecular variants. *J Clin Oncol.* 2011; 29:1408–1414. Epub 2010 Sep 1407. [PubMed: 20823417]
47. Spatz A, Borg C, Feunteun J. X-Chromosome Genetics and Human Cancer. *Nat Rev Cancer.* 2004; 4:617–629. [PubMed: 15286741]
48. Lindqvist L, et al. Selective Pharmacological Targeting of a DEAD Box RNA Helicase. *PLoS One.* 2008; 3:e1583. [PubMed: 18270573]
49. Engelman JA. Targeting PI3K signalling in cancer: opportunities, challenges and limitations. *Nat Rev Cancer.* 2009; 9:550–562. [PubMed: 19629070]
50. Zhang J, et al. The genetic basis of early T-cell precursor acute lymphoblastic leukaemia. *Nature.* 2012; 481:157–163. [PubMed: 22237106]

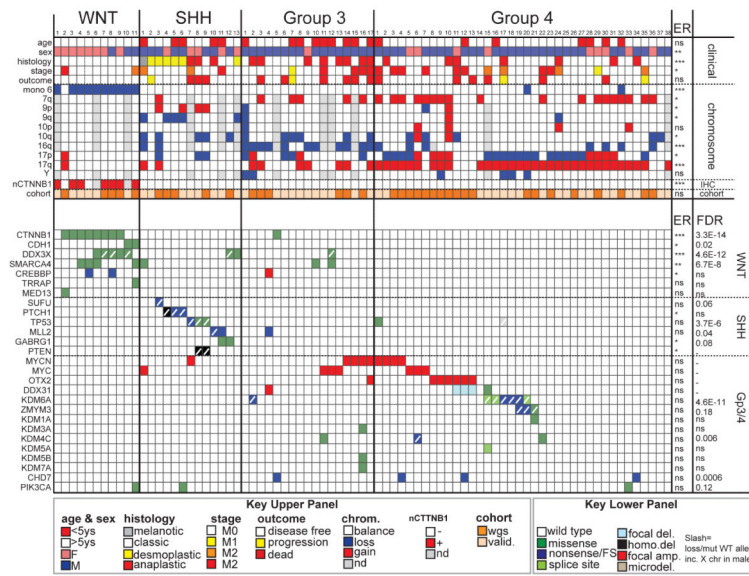


**Figure 1. The genomic landscape of medulloblastoma**

Top: clinical, histologic, gross chromosomal, nuclear CTNNB1 (nCTNNB1), and cohort (discovery or validation) details of 79 medulloblastomas by subgroup. Below: genetic alterations detected in 27 genes of particular interest. Color key at bottom. ANOVA (continuous) or Fisher’s exact (categorical) p-value is shown right. False discovery estimates (FDR) of each mutation are shown right. \*\*\*=P<0.0005; \*\*=P<0.005; \*=P<0.05; ns=not significant.

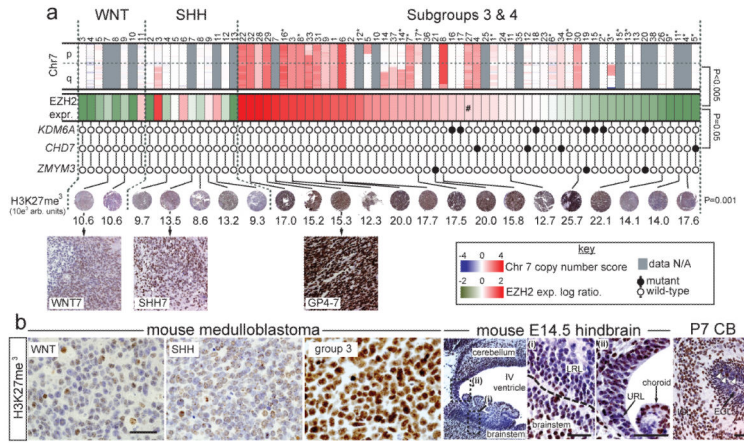


**Figure 2. Deregulation of H3K27me3 in subgroup-3 and 4 human and mouse medulloblastoma**  
**(a)** Top row, SNP profiles of chromosome 7 copy number in medulloblastomas (samples as Figure 1; \*=subgroup-3 cases). Second row, expression of EZH2. Subgroup-3 and 4 tumours are ordered left to right by expression level, #=median expression point (Bonferroni corrected p-value of EZH2 expression vs. chromosome 7 gain). Third row, mutation status of *KDM6A*, *CHD7* and *ZMYM3* (p-value, Fisher’s exact mutations vs. EZH2 expression). Fourth row, H3K27me3 immunohistochemistry (numbers=colorimetry, p-value ANOVA).  
**(b)** H3K27me3 expression (right) in mouse *Blbp-Cre ; Ctnnb1<sup>+lox(Ex3)</sup> ; Tp53<sup>flx/flx</sup>* (WNT), *Ptch1<sup>+/-</sup> ; Tp53<sup>-/-</sup>* (SHH) and *Myc ; Ink4c<sup>-/-</sup>* (group 3) medulloblastomas and (left) developing hindbrain. high power views of E14.5 (i) LRL and (ii) upper rhombic lip (URL). IGL=internal granule layer, EGL=external germinal layer. Scale bar=50µm. White arrows in P7 cerebellum pinpoint H3K27me3 cells in the EGL.



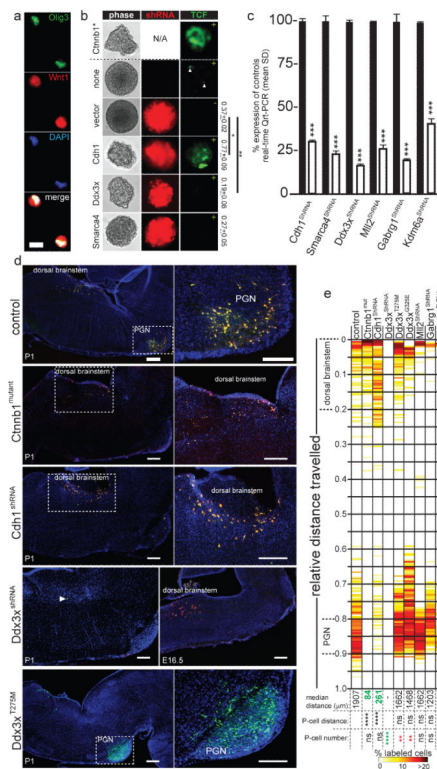


**Figure 3. Genes mutated in WNT-subgroup medulloblastomas regulate LRLPs**  
**(a)** Isolated Olig3<sup>+</sup>/Wnt1<sup>+</sup> LRLPs were transduced in **(b)** with mutant Ctnnb1 (above hashed line) or the indicated shRNA-Red Fluorescence Protein construct (below hashed line). LRLPs were also transduced (+) or not (-) with a Tcf-Lef-enhanced green fluorescence (Tcf) reporter. Numbers right report clonal % 2' to 3' passage neurosphere formation (+SD). **(c)** Knock-down of genes targeted by shRNA relative to control transduced cells. **(d)** Immunofluorescence of P1 mouse hindbrains electroporated *in utero* at E14.5 with GFP (to control for equivalence of electroporation between embryos control) and the indicated construct. High-power views of indicated areas are shown right. Cells targeted by Ddx3x-shRNA are present 48 hours post electroporation but ablated by P1. Scale=200µm. **(e)** Heatmap reporting the distribution of GFP<sup>+</sup>/RFP<sup>+</sup> cells in electroporated mice at P1. Median distance migrated by cells, and p-values of migration distance and cell number relative to controls is shown (\*\*\*\*, p<0.00005; \*\*\*, p<0.0005; \*\*, p<0.005; \*, p<0.05. Red and green text reports significant increase or decrease, respectively relative to control).

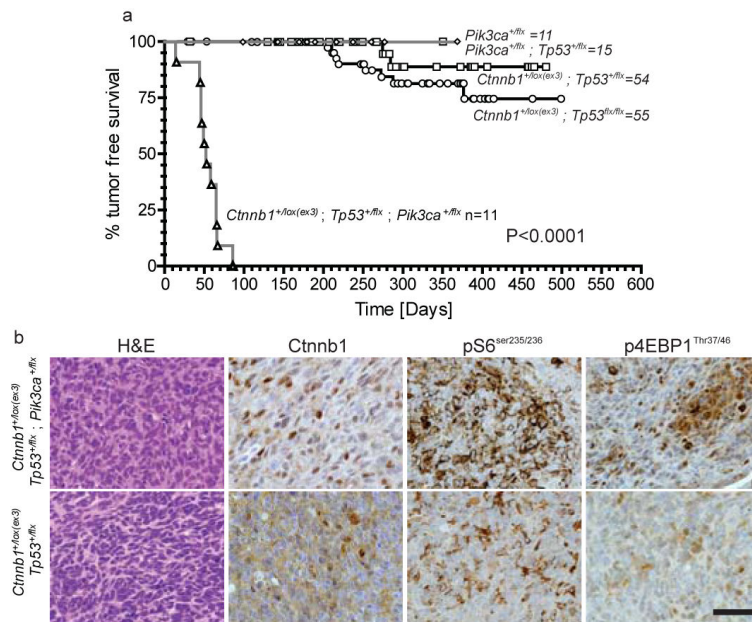


**Figure 4.** *Pik3ca<sup>E545K</sup>* accelerates but does not initiate WNT-subgroup medulloblastoma Tumour free survival of mice of the indicated genotype. All mice carry the *Blbp-cre* allele. Log Rank  $P < 0.0001$ . **(b)** Hematoxylin and eosin and immunohistochemical stains of indicated tumors. Scale=50  $\mu$ m.